

# Supplementary material for “Impact of differential stress on fracture due to volume increasing hydration”

Jeremiah J. McElwee<sup>1</sup>, Ikuko Wada<sup>1</sup>, Kazuki Yoshida<sup>2</sup>, Hiroyuki Shimizu<sup>3</sup>, Atsushi Okamoto<sup>4</sup>

<sup>1</sup>Department of Earth and Environmental Sciences, University Minnesota Twin Cities, Minneapolis, 55406, USA

<sup>2</sup>Institute of Materials Structure Science, High Energy Accelerator Research Organization, Tsukuba, 305-0801, Japan

<sup>3</sup>Geotechnical Analysis Group, Advanced Analysis Department, Civil Engineering Design Division, Kajima Corporation, Tokyo, Japan

<sup>4</sup>Graduate School of Environmental Studies, Tohoku University, Miyagi, 980-8578, Japan

Correspondence to: Jeremiah J. McElwee (mcelw020@umn.edu)

## S1 Inferring Young's Moduli from the Stress-Strain Curves

To quantify the macroscopic properties (**Table 1**) that result from the microscopic parameters described in the Methods section, we performed uniaxial compression and tension test simulations (**Fig. S1**). These simulations were run on models made up of fully unreacted and fully reacted disks. Plane strain was assumed when calculating elastic parameters from the simulations. To calculate Young's modulus, the tangent of the initial slope of the stress-strain curves was used so as to match dynamic Young's moduli calculated from acoustic experiments (*Christensen, 2004*) and because the DEM does not exhibit noise during initial loading, as is commonly a concern in laboratory experiments. For details on how the uniaxial compression and tension simulations are conducted, and for how stress and strain is measured in these simulations, see *Okamoto and Shimizu (2015)* and *Shimizu and Okamoto (2016)*. The obtained macroscopic properties values (**Table 1**) are in good agreement with those reported by *Okamoto and Shimizu (2015)* and *Shimizu and Okamoto (2016)*.

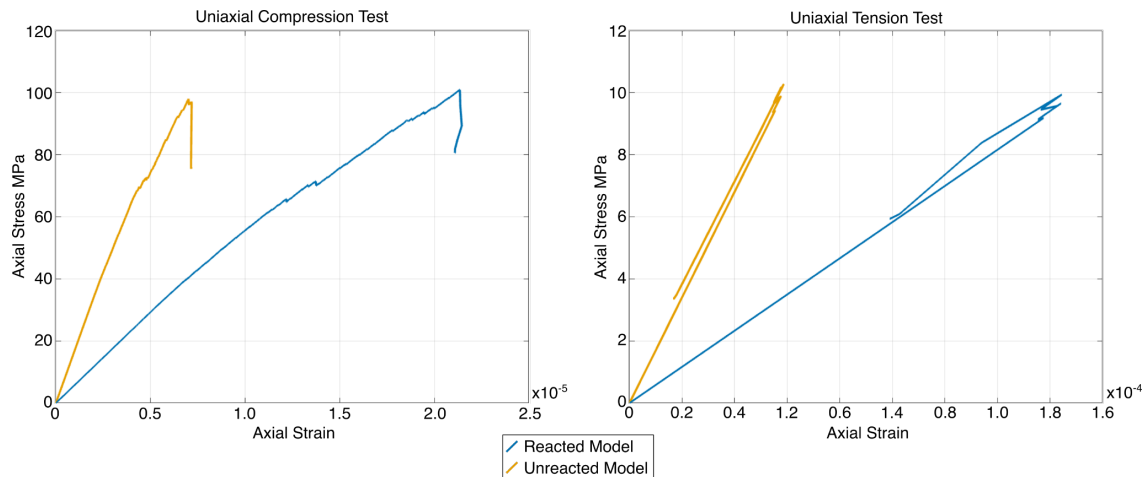


**Figure S1: Stress-strain relations for plots of models with reacted disks (blue lines) and unreacted disks (blue lines) models subjected to (a) uniaxial compression and (b) uniaxial tension.**

## S2 Effects of Inertia Cracks

To find a reaction rate that results in a stable solution under differential stress, we ran simulations with varying reaction rates under horizontal compression ( $(\sigma_x - \sigma_y) = 10$  MPa). These simulations had a similar setup to those in the main text except that the unreactive layer at the base of the model was excluded, the simulations were run at a higher confining pressure of 5 MPa, and  $\psi_m$  and  $\psi_f$  were 10 and 100000, respectively. The results of those simulations show that the crack density loses its dependence on  $Z_{max}$  when  $Z_{max} \leq 25$  s<sup>-1</sup>, indicating that inertial cracks are minimized for those  $Z_{max}$ . However, when  $Z_{max}$  is less than 25 s<sup>-1</sup>, the ratio of shear to tensile cracks in the simulations increases with decreasing  $Z_{max}$  and becomes stable when  $Z_{max}$  is below 5 s<sup>-1</sup> (Fig. S2). To minimize this effect and ensure a stable solution, we choose  $Z_{max} = 5$  s<sup>-1</sup> for the simulations in the main text. We note that a series of simulations run with constant  $Z_{max}$  but varying time step magnitudes indicate that the above dependence of the shear to tensile crack ratio on  $Z_{max}$  is independent of the time step size.

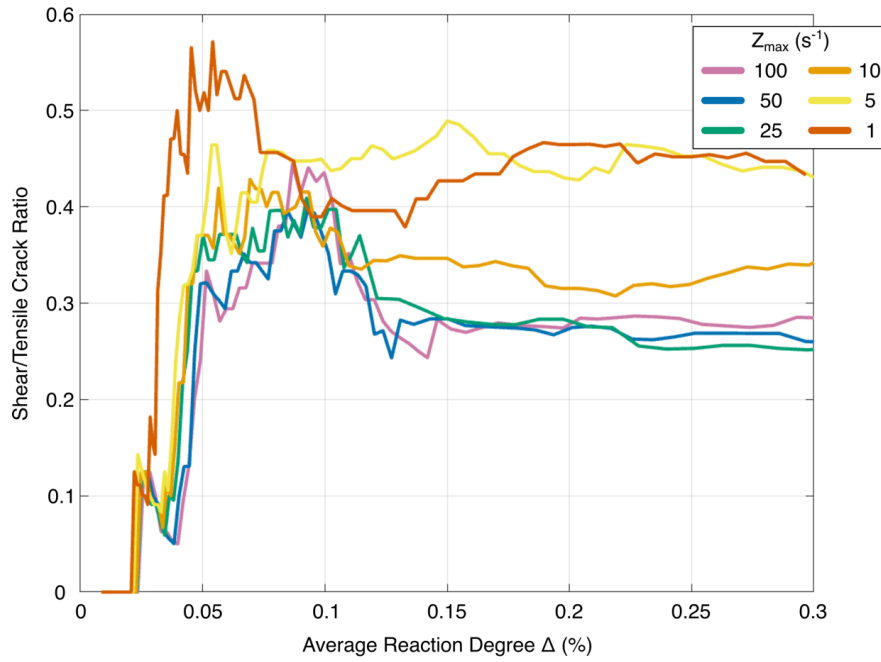


**Figure S2: Ratio of shear to tensile cracks with the average reaction degree ( $\Delta$ ) for models at different maximum reaction rates. Note that, for  $\Delta > 0.15\%$ , the ratio of shear to tensile cracks loses its  $Z_{max}$  dependence when  $Z_{max}$  is small ( $\leq 5$  s<sup>-1</sup>).**

## S3 Effects of Model Dimensions

The model dimensions in this study were 5 mm  $\times$  5 mm. To test the effect of the height of the model domain, simulations were run at  $(\sigma_x - \sigma_y) = 0, 2, 5$ , and 10 MPa with 10-mm-high model domains (Fig. S3) and compared to results from the 5-mm-high models discussed in the main text. In the compressive simulations in the main text, a reacting layer characterized by spalling develops at the base of the model before the model transitions to longer tensile fractures at high angles to the base of the model when the reacting layer reaches some thickness. The models with varying aspect ratios indicate that the thickness of this layer before the transition to branching fracture increases with lateral compressive stress and the height of the model. This is consistent with previous modeling results that indicate the transition from spalling to branching depends on the domain size (Ulven *et al.*, 2014a; Iyer *et al.*, 2008) and with arguments from elasticity (Timoshenko and Moreno, 1970). In the 5-

and 10-mm-high models under the hydrostatic condition, the branching pattern develops immediately without the development of a reacting layer. Therefore, the fracture pattern under hydrostatic stress and deviatoric tension can be thought of as an end member with a reacting layer thickness of 0.

50 Although the fracture style is the same in the 5- and 10-mm-high hydrostatic models, the volume of fluids channeled into the model is much larger in the 10-mm-high model because the cracks can be longer. As a result, after the first tensile cracks connect to the base of the model, the average reaction rate of the whole model becomes much faster than in the models under lateral compression. The 5-mm-high models show a model reaction rate similar to the lateral compression models because the tensile cracks are limited by the boundaries of the model. Because of this effect of model size on the flow rate, we do not directly  
55 compare the magnitude of flow rates into the model domain for each stress condition in the main text. Instead, we focus on changes in the flow rate through time.

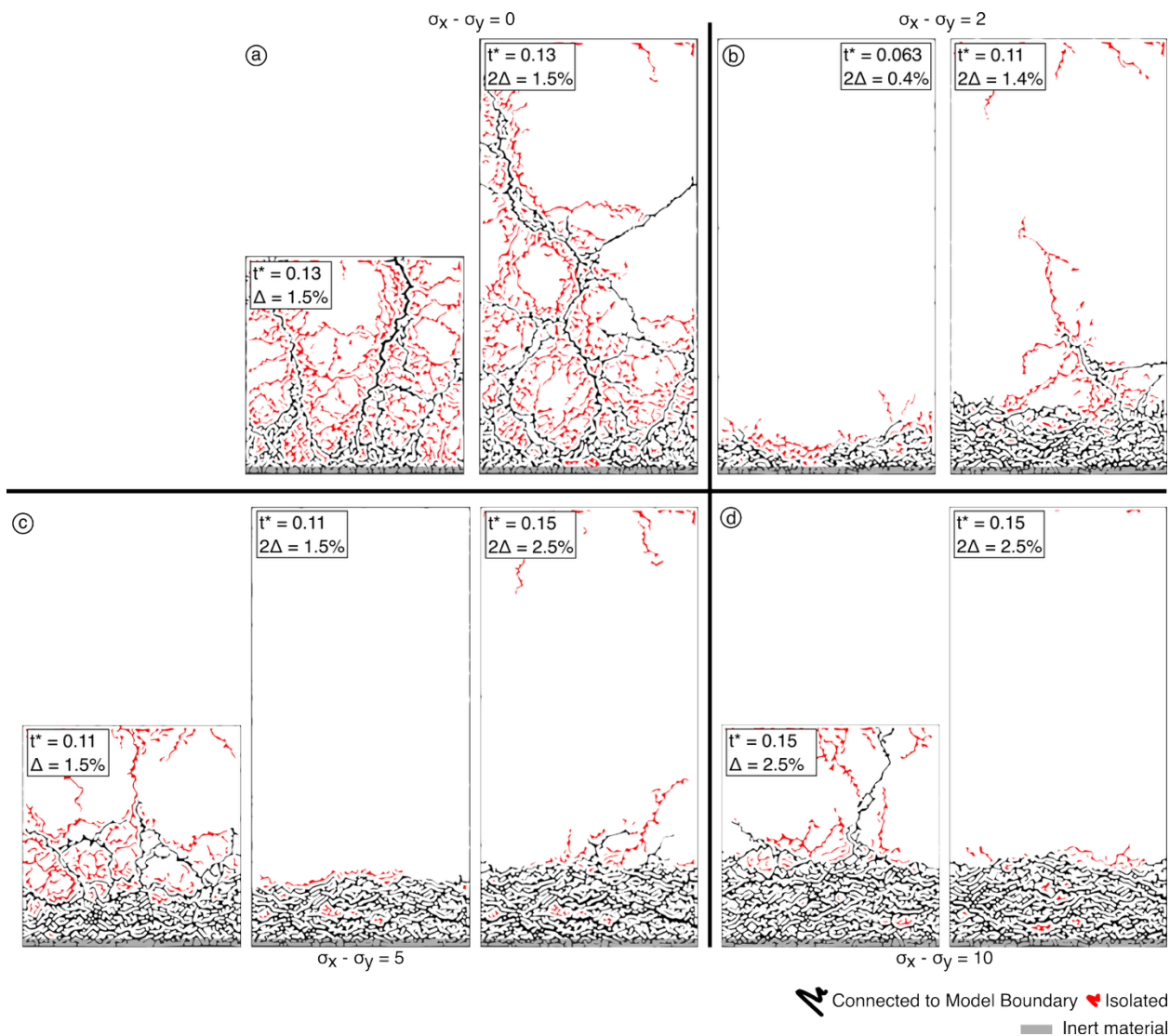


Figure S3: The effect of model domain height under (a) hydrostatic, (b) horizontal compression of 2 MPa, and (c) horizontal compression of 5 MPa, and (d) horizontal compression of 10 MPa. Square models for the hydrostatic case, the 5 MPa horizontal compression case, and the 10 MPa horizontal compression case are included for comparison. Black and red paths indicate cracks that are connected to and isolated from the model boundaries, respectively. Models run under lateral compression exhibit a fractured front  
60

at the base of the model domain before developing branching tensile cracks in the interior. With increasing lateral compression and increasing model height, the thickness of the reactive fractured layer increases prior to tensile cracking.

#### S4 Models with Higher Matrix Permeability

65 We tested the effect of permeability on the models by running simulations under deviatoric tension ( $\sigma_x - \sigma_y = -10$ ), a hydrostatic condition ( $\sigma_x - \sigma_y = 0$ ), and deviatoric compression ( $\sigma_x - \sigma_y = 10$ ) with matrix permeabilities ten times higher than in the main text ( $\psi_m = 10$  here). The results indicate that high matrix permeability limits spalling, leading to larger subdomains of the unreacted interior via branching. In all three simulations, spalling was much less prevalent than in the low permeability models in the main text. Less spalling is consistent with the results in **Text S3** because high permeability results in a  
70 thicker reacting layer relative to the unreacted interior, which promotes branching. In the deviatoric tension case, high permeability also limits spalling parallel to long tensile cracks. The anticorrelation between spalling and matrix permeability was explored in *Ulven et. al. (2014b)* and our results here are consistent with what they report.

Additionally, in the hydrostatic and deviatoric tension models, the subdomains created by branching fractures were larger than in the low permeability models in the main text. This may be because there was less spalling, which encroaches on  
75 the unreacted subdomains. Alternatively, it may be because less fracture occurred in general. High matrix permeability results in low reaction-induced strain gradients. Given that cracking occurs due to strain gradients, the end result of higher matrix permeability is fewer cracks and larger subdomains. End member simulations in *Shimizu and Okamoto (2016)* indicate that very little cracking occurs when the matrix permeability is too high, and that, up to the endmember permeability, the amount of cracking decreases with increasing permeability.

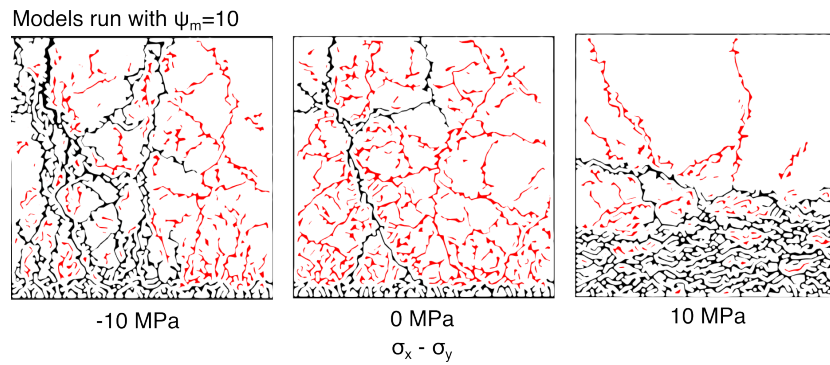


**Figure S4: Simulations run with a higher matrix permeability ( $\psi_m = 10$ ). Left: horizontal deviatoric tension. Center: hydrostatic condition. Right: horizontal deviatoric compression. Black and red paths indicate cracks that are connected to and isolated from the model boundaries, respectively.**

85

## References

- Christensen, N. I.: Serpentinites, peridotites, and seismology, *International Geology Review*, 46, 795–816, <https://doi.org/10.2747/0020-6814.46.9.795>, 2004.
- 90 Iyer, K., Jamtveit, B., Mathiesen, J., Malthe-Sørenssen, A., and Feder, J.: Reaction-assisted hierarchical fracturing during serpentization, *Earth and Planetary Science Letters*, 267, 503–516, <https://doi.org/10.1016/j.epsl.2007.11.060>, 2008.
- Okamoto, A. and Shimizu, H.: Contrasting fracture patterns induced by volume-increasing and -decreasing reactions: Implications for the progress of metamorphic reactions, *Earth and Planetary Science Letters*, 417, 9–18, <https://doi.org/10.1016/j.epsl.2015.02.015>, 2015.
- 95 Shimizu, H. and Okamoto, A.: The roles of fluid transport and surface reaction in reaction-induced fracturing, with implications for the development of mesh textures in serpentinites, *Contributions to Mineralogy and Petrology*, 171, 1–18, <https://doi.org/10.1007/s00410-016-1288-y>, 2016.
- Timoshenko, P. S., Goodier, J.N.: *Theory of Elasticity*, third edition. McGraw-Hill, New York. ISBN 07-064720-8, 1970
- Ulven, O. I., Jamtveit, B., and Malthe-Sørenssen, A.: Reaction-driven fracturing of porous rock, *Journal of Geophysical Research: Solid Earth*, 119, 7473–7486, <https://doi.org/10.1002/2014JB011102>, 2014a.
- 100 Ulven, O. I., Storheim, H., Austrheim, H., and Malthe-Sørenssen, A.: Fracture initiation during volume increasing reactions in rocks and applications for CO<sub>2</sub> sequestration, *Earth and Planetary Science Letters*, 389, 132–142, <https://doi.org/10.1016/j.epsl.2013.12.039>, 2014b.